ORIGINAL RESEARCH

Food grade titanium dioxide disrupts intestinal brush border microvilli in vitro independent of sedimentation

James J. Faust · Kyle Doudrick · Yu Yang ·
Paul Westerhoff · David G. Capco

Abstract Bulk- and nano-scale titanium dioxide (TiO_2) has found use in human food products for controlling color, texture, and moisture. Once ingested, and because of their small size, nano-scale TiO_2 can interact with a number of epithelia that line the human gastrointestinal tract. One such epithelium responsible for nutrient absorption is the small intestine, whose constituent cells contain microvilli to increase the total surface area of the gut. Using a combination of scanning and transmission electron microscopy it was found that food grade TiO_2 (E171 food additive coded) included ~25 % of the TiO_2 as nanoparticles (NPs; <100 nm), and disrupted the normal organization of the microvilli as a consequence of TiO_2 sedimentation. It was found that TiO_2 isolated from the candy coating of chewing gum and a commercially available TiO_2 food grade additive samples were of the anatase crystal structure. Exposure to food grade TiO_2 additives, containing nanoparticles, at the lowest concentration tested within this experimental paradigm to date at 350 ng/mL (i.e., 100 ng/cm^2 cell surface area) resulted in disruption of the brush border. Through the use of two independent techniques to remove the effects of gravity, and subsequent TiO_2 sedimentation, it was found that disruption of the microvilli was independent of sedimentation. These data indicate that food grade TiO_2 exposure resulted in the loss of microvilli from the Caco-2$_{BBe1}$ cell system due to a biological response, and not simply a physical artifact of in vitro exposure.

Keywords Brush border · Microvilli · Nanotechnology · Sedimentation · Titanium dioxide · Toxicity

Abbreviations
BBe1   Brush border expressing 1
ICP-MS   Inductively coupled plasma mass spectroscopy

J. J. Faust · D. G. Capco (✉)
Molecular and Cellular Biosciences, School of Life Sciences,
Arizona State University,
Tempe, AZ 85287-4501, USA
e-mail: Dcapco@asu.edu

K. Doudrick · Y. Yang · P. Westerhoff
School of Sustainable Engineering and the Built Environment,
Arizona State University,
Tempe, AZ 85287-5306, USA

Introduction

TiO_2 has found use as a color additive in human food products because of its brilliant white color, and as a texture modifier in foods, which is used in a wide variety of confectionary foods, toothpastes, and other ingestible products. "E" numbers are codes for substances that can be used as food additives in the European Union, and similar coding exists in other countries; food grade TiO_2 is coded as E171. In the USA, the Food and Drug Administration approved the use of TiO_2 in 1966 as a human food additive with the stipulation that TiO_2 is not to exceed 1 % by weight (Regulations 2000). While

TiO$_2$ has been approved, the study by Weir et al. showed that approximately 38 % of TiO$_2$ in one food grade (E171 coded) source had at least one external dimension that was <100 nm, which was consistent with the size distribution observed in several food samples containing TiO$_2$, including confectionary products (e.g., chewing gum) or toothpastes (Weir et al. 2012). These data indicate that a subset of TiO$_2$ approved as additives in human food products is within the accepted definition of nanomaterial (Dunphy Guzman et al. 2006), yet little information on the toxicity of food grade TiO$_2$ has been published since these definitions for nanotechnology have been established.

Although there is clearly a beneficial niche for the use of TiO$_2$ as a food additive, it is coming to the attention of investigators that although not immediately damaging to an epithelium, TiO$_2$ NPs elicit subtle effects on cells within an epithelium (Koeneman et al. 2010). An epithelium has a barrier function that partitions parts of the body and even separates the body from the external environment. The study by Koeneman et al. (2010) indicated that exposure to a 70/30 % mixture of rutile/anatase TiO$_2$ NPs result in what appeared to be a dose-dependent disruption of the brush border, an anatomical feature that exists on the epithelial surface of absorptive cells of the intestine. These data have been corroborated by a number of brush border expressing cell models with another widely employed model NP, α-Fe$_2$O$_3$ (Faust et al. 2014b; Zhang et al. 2010; Kalive et al. 2012). Although the entire picture has yet to be painted, the role of many molecular components of the brush border composed of individual microvilli have been elucidated (Bement and Mooseker 1996; Mooseker 1985). Briefly, the brush border has been partitioned into two regions that make up the apical portion of the enterocyte in the epithelium: The microvilli and terminal web domains. Within the microvilli domain, the single microvillus has 20–30 actin filaments organized as parallel bundles in a hexagonal array (Bretscher 1983). Each actin filament is fastened to the other by fimbrin, villin, and espin (Bretscher and Weber 1980a, b; Grimm-Günter et al. 2009). The entire microvillus core is laterally tethered in a helical arrangement to the overlying plasma membrane by brush border myosin I (Howe and Mooseker 1983). The microvilli are rooted in the terminal web which is composed of a number of intermediate filaments and structural proteins (Hirokawa et al. 1983; Hirokawa and Heuser 1981).

The study by Zhang et al. (2010) postulated that adsorption of NPs to the cell surface results in disruption of the brush border. In line with this view, at least one criticism of the in vitro culture model is the fact that as NPs agglomerate over time sedimentation ensues and effectively increases the concentration of NPs at the bottom of the culture dish that the cells would otherwise not be exposed to (Cho et al. 2011). This increase in NP concentration at the apical surface of the cell could result in artifactual disruption of the brush border. Therefore, the current study was conducted in order to determine if exposure to food grade TiO$_2$ (labeled as E171 compliant by the distributor) as well as TiO$_2$ isolated from the candy coating of gum (hereafter referred to as gum TiO$_2$) resulted in brush border disruption, and if this disruption was a result of sedimentation. In this study it was hypothesized that brush border disruption occurs as a result of exposure to food grade TiO$_2$ and that brush border disruption is an event independent of sedimentation. If TiO$_2$ disrupts the brush border, then changes will occur as a result of exposure to food grade TiO$_2$ as measured by an alteration in the archetypical organization of the brush border as well as a reduction in the total number of microvilli. Furthermore, if brush border disruption is independent of sedimentation, then removing the effects of sedimentation due to gravity should result in disruption of the brush border as measured by an alteration in the archetypical organization of the brush border as well as a reduction in the total number of microvilli.

Methods

TiO$_2$ isolated from candy coatings, and preparation of culture medium containing TiO$_2$

E171 is a European Union designation for a white food color additive that is known elsewhere by other designations (CI 77891, Pigment White 6). For this research, a sample was obtained from a large commercial supplier in China, which listed the material as complying with E171 requirements (referred to in this study as food grade TiO$_2$). Food grade TiO$_2$ was suspended in sterile Nanopure™ water (Barnstead; 18.2 MΩ) at a concentration of 1 mg/mL. TiO$_2$ was also isolated from gum (referred to in this study as gum TiO$_2$) as described by Weir et al. (2012). Briefly, three servings of gum were added to 5 mL of sterile Nanopure™ water (Barnstead;

18.2 MΩ) and allowed to dissolve for 10 min. In order to determine the total Ti content in food grade TiO_2 and gum TiO_2, approximately 0.03 g of each was digested in HNO_3 and HF (4:1 v/v) using microwave digestion according to Standard Method 3030G (APHA et al. 2005). Element concentrations including Ti, P, Si, and Al were measured using XSERIE-2 ICP-MS (Thermo Scientific, USA). The total amount of Ti from this stock concentration was determined by ICP-MS before the samples were used in any other experiment. Before the TiO_2 was resuspended in cell culture medium, the TiO_2 was sonicated with a Fisher Scientific model 100 probe sonic dismembrator at the maximum setting of 28 watts (root mean square, RMS) for no less than 2 min. The TiO_2 was diluted to the final working concentration and sonicated a second time with a Fisher Scientific model 100 probe sonic dismembrator at the maximum setting of 28 watts (RMS) for no less than 2 min. In this study, concentrations are shown as mass per milliliter. It should be noted, however, that the cell culture device has a growth surface area of 3.5 cm^2 and the epithelium forms a confluent layer across this growth area. Consequently, when 1 mL of culture medium containing 350 ng TiO_2 is placed above this growth area, the concentration is 350 ng/mL which is equal to 100 ng/cm^2 of TiO_2 available to the epithelia.

XPS

Surface elemental composition and chemical state were analyzed using X-ray photoelectron spectroscopy (XPS) performed on an ESCALAB 220i-XL (Vacuum Generators, USA) with a monochromatic Al Kα source at hν=1486 eV, a base pressure=$7×10–10$ mbar, and a spot analysis size of 500 μm. Food grade TiO_2 was prepared by pressing the powder into a disk on clean indium foil. Gum TiO_2 was prepared by drop casting the isolated suspension onto SiO_2. Peak fit was done manually using CasaXPS on the basis of the theoretical atomic percentages calculated from the wide scan. The estimated depth of analysis is approximately 2.87 nm as determined from the inelastic mean free path of electron scattering for TiO_2 (Tanuma et al. 1994). The adventitious carbon peak was used for calibration.

XRD

The crystal structure was determined using powder X-ray diffraction (XRD) on a D5000 (Siemens, USA) with a CuK_α source and an aluminum holder. Each sample was scanned from 2θ=20° to 60° to detect the characteristic TiO_2 peaks. The XRD spectrum was used to calculate the lower bound of the crystallites using Scherrer's Equation (Patterson 1939). Surface elemental composition and chemical state were analyzed using X-ray photoelectron spectroscopy (XPS) performed on a ESCALAB 220i-XL (Vacuum Generators, USA) with a monochromatic Al K$_\alpha$ source at hν=1486 eV and a base pressure=$7×10^{-10}$ mbar. XPS spectra were calibrated using the O 1s peak for TiO_2 at 530.1 eV.

TEM and primary particle diameter analysis

Food grade and gum TiO_2 samples were diluted to 1 μg/mL in Nanopure™ water (Barnstead; 18.2 MΩ) and sonicated with a Fisher Scientific model 100 probe sonic dismembrator at the maximum setting of 28 watts (RMS) for no less than 2 min. Small (10 μL) drops containing the titanium dioxide were placed on Parafilm. Formvar-coated copper grids were inverted and immediately placed on top of the drops for 10 s. The excess liquid was wicked away with Whatman no. 5 filter paper, and the grids were placed in a grid holder over night to dry before imaging with a Philips CM-12 TEM. Images were captured by randomly focusing on five different squares within the mesh of three different grids. Each of the micrographs (15 in total) were analyzed with ImageJ by measuring the x and y axis of the TiO_2 and averaging the diameter from every particle within the field of view. In total 100 particles were averaged, and the data was found to be consistent with those results reported elsewhere (Weir et al. 2012).

Dynamic light scattering

Samples were prepared for phase analysis light scattering (ZetaPALS, Brookhaven Instruments Corporation, U.S.) to determine the hydrolyzed diameters of particles by application of 10 mg/L TiO_2 samples in Nanopure™ water and bath sonicating for 30 min. The aforementioned protocol was employed also to analyze particles in the presence of cell culture medium containing serum. Preliminary experiments indicated that there was no significant change in hydrodynamic diameter for either of the sonication methods employed in the present investigation (i.e., bath sonication for 30 min compared to probe sonication for no less than 3 min).

Zeta potential analysis

In order to determine the zeta potential, the electrode was stabilized in 100 mM potassium nitrate at room temperature 24 h prior to measurement. The samples were prepared by adding 0.03 g of food grade TiO_2 or gum TiO_2 to 50 mL of 10 mM potassium nitrate (Sigma-Aldrich, U.S.) solution, which was mixed for 24 h. After this time period, the samples were bath sonicated for 30 min immediately before zeta potential measurements.

Cell culture

This study exploits the use of the extensively characterized Caco-2$_{BBe1}$ human derived cell system. When grown appropriately, this cell system exhibits a faithful representation of the in vivo structural characteristics (Peterson and Mooseker 1992), and mirror differentiation of the brush border at the molecular level (Peterson and Mooseker 1993). Furthermore, Caco-2 has been recommended by the International Life Sciences Institute Research/Risk Science Institute (ILSI RF/RSI; Oberdörster et al. 2005). The human, brush border expressing cell line, Caco-2$_{BBe1}$, was cultured according to the protocol established elsewhere (Peterson and Mooseker 1992). Briefly, Caco-2$_{BBe1}$ cells were purchased from ATCC (Manassas, VA; CRL-2102) at passage 47 and discarded at passage 67. The cell culture medium is Dulbecco's modification of Eagle's medium (DMEM; Cellgro; 10-017-CM) supplemented with 10 μg/mL of human transferrin (Invitrogen; 0030124SA), 10,000 I.U./mL penicillin, 10,000 μg/mL streptomycin and 25 μg/mL amphotericin (Cellgro; 30-004-CI), as well as 10 % fetal bovine serum (Biosera; FBS2000). The cell culture medium was replenished every 48 h, and culture vessels containing the cells were housed in a humified incubator calibrated to maintain an atmosphere of 5 % CO_2 at 37 °C. The experiments were conducted only after the cells were aseptically maintained as confluent epithelia for 19–21 days (Peterson et al. 1993), where replicate samples had an electrical resistance of at least $250\Omega/cm^2$ and ZO-1 is apically localized.

Electron microscopy

Preparation of Caco-2$_{BBe1}$ epithelia for electron microscopy was conducted according to a detailed protocol (Faust et al. 2014a). Briefly, specimens were grown for 19–21 days, the experiment conducted, and the specimens were fixed for 1 h at room temperature in 2 % glutaraldehyde made in 100 mM sodium cacodylate buffer (pH 7.2). The specimens were washed and post-fixed for 1 h at room temperature in 1 % OsO_4 made in 100 mM sodium cacodylate buffer (pH 7.2). The specimens were dehydrated, and either critical point dried and sputter coated, or infiltrated with Spurr's resin. Images were procured with either an XL-30 ESEM coupled with EDX analytical software, or a JOEL JSM-6300 equipped with an IXRF digital imaging system. TEM micrographs were procured with a Phillips CM-12 fitted with a Gatan 791 CCD camera. The images shown are representative micrographs from five randomly chosen cells of three independent experiments.

Procedure for the inversion of specimens to remove the effects of sedimentation of TiO_2 on the surface of the epithelium

The human, brush border expressing cell line, Caco-2$_{BBe1}$, was cultured according to the protocol described the in the Cell culture section. After the 19–21 days necessary to permit differentiation of the epithelia, the epithelia were transferred to 15-mL conical centrifuge tubes (VWR; 89039–664) containing no culture medium, the side facing the epithelia were labeled, and 5 mL of medium was added to the centrifuge tubes while the epithelia remained inverted. The specimens were returned to the cell culture incubator with the cap of the 15-mL centrifuge tube tightened half way to permit exchange of gas. At the indicated time points, the specimens were removed and maintained in the inverted position, the cell culture medium was aspirated with the epithelia remaining inverted, and the cytological fixative was added while the specimens were inverted. Only after 1 h of fixation were the specimens handled in any other orientation.

Videomicroscopy

Caco-2$_{BBe1}$ epithelia were cultured on μ-Dish$^{35\ mm,\ high}$ glass bottom Grid-50 dishes (Ibidi; 81148) according to the aforementioned cell culture protocol. Prior to examination, medium containing the food grade TiO_2 was prepared according to the method of Koeneman et al.

([2010](#)). Briefly, concentrated, TiO_2 stocks (no less than 500 mg/L) were thoroughly sonicated with a Fisher Scientific model 100 probe sonic dismembrator at the maximum setting of 28 watts (RMS) for no less than 2 min. This TiO_2 suspension was subsequently dosed at a working concentration of 1 $\mu g/cm^2$ of surface area (i.e., 3.5 $\mu g/mL$), sonicated a second time, and bath applied to the epithelia. Immediately following exposure to this TiO_2-containing medium, the cells were imaged with a Nikon Eclipse TE300 inverted microscope equipped with a stage warmer and a Hamamatsu Orca CCD camera. For experiments conducted without cells, the TiO_2 were applied at a 1 $\mu g/cm^2$ (3.5 $\mu g/mL$) concentration to a gridded glass bottom dish that contained 50 $\mu g/cm^2$ collagen I. The TiO_2 were visualized by micropipetting the appropriate stock TiO_2 volume corresponding to 1 $\mu g/cm^2$ to the center of the field of view while imaging live. The cell culture medium was washed two times with Nanopure™ water (Barnstead; 18.2 MΩ), a still frame corresponding to the same region was captured, and the water was decanted and allowed to air dry overnight. The following day (12 h later), the surrounding region that was imaged live was scored with a diamond-tipped glass cutter, immobilized on an aluminum stub, and sputter coated with gold. The same region that was imaged with the phase contrast microscope live was imaged with an FEI XL-30 ESEM equipped with EDX elemental analysis.

Procedure for culturing Caco-2$_{BBe1}$ epithelia under conditions of microgravity

The human, brush border expressing cell line, Caco-2$_{BBe1}$, was cultured according to the protocol described the in the Cell culture section. The epithelia were cultured 19–21 days to permit differentiation of the epithelia and subsequently transferred to disposable rotary cell culture vessels (Synthecon; D-410), and microgravity was engaged through the use of a microgravity bioreactor (Synthecon; RCCS-4) with the controller set to 24.3 RPM. After microgravity was obtained, as evidenced by "floating" epithelia in the center of the disk, the NP-containing medium was perfused into the chamber and permitted culture for 24 h in a cell culture incubator. The specimens were fixed while maintaining microgravity for 1 h at room temperature prior to removing the epithelia from the disk.

Data analysis

In this manuscript, an experiment is defined as at least replicate samples for each treatment with the respective controls conducted on three different days (i.e., at least technical duplicate with three biological replicates). The number of microvilli and the organization of the brush border were analyzed by randomly imaging at least three micrographs from each replicate sample. Random 1-μm^2 squares were generated through the use of Powerpoint and the number of microvilli within the 1-μm^2 squares were counted from at least three random squares in a single micrograph. The three to five regions were averaged, and the data from the three experiments were compiled to generate an average. Error was determined with Excel and shown as standard error of the means. Multiple comparisons were accomplished via one-way ANOVA with either Dunn's or Tukey posttests. Data were considered significant if $p < 0.05$. If untreated specimens appeared in poor health, the entire experiment, including those epithelia exposed to the TiO_2 was culled from analysis.

Results

Material characterization

Thorough characterization of the two TiO_2 samples was conducted to provide information on their size, morphology, and chemical composition, for which little information exists in open peer-reviewed literature on food grade TiO_2. TEM analysis revealed that food grade and gum TiO_2 are colloidal scale and have spherical to a slightly longer aspect ratio geometry (Fig. [1a, b](#)). The primary particle diameters for food grade and gum TiO_2 were 122±48 and 141±56 nm in any external dimension, respectively. There were a range of primary particle diameters (longest dimension) from 51 to 290 nm, and 48.5 to 305 nm for food grade and gum TiO_2, respectively. The food grade and gum TiO_2 samples contained 23 and 23 % of nano-scale particles upon the size distributions with a confidence level of 95 %, respectively, based on counting 100 particles sampled from a total of 10,000 particles. Separate phase analysis light scattering for food grade TiO_2 and gum TiO_2 conducted on an ultrapure water solution containing TiO_2 at a concentration of 10 mg/L indicated the mean (±standard deviation) hydrodynamic diameter was 220

Fig. 1 Transmission electron micrographs of food grade TiO$_2$ (**a**; identified as E171 compliant) and **b** gum TiO$_2$. The *scale bar* in the *lower right corner* of the micrographs is 200 nm
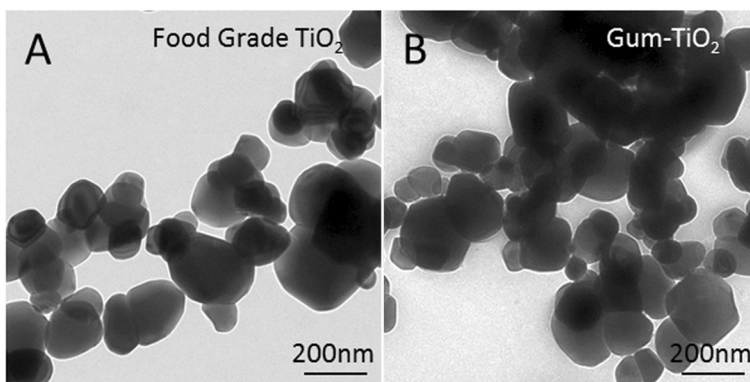
±9 nm (polydispersity=0.130±0.013) and 250±10 (polydispersity=0.165±0.014), respectively. In additional, light scanning for food grade TiO$_2$ and gum TiO$_2$ was conducted in serum-containing cell culture medium. When the samples were bath sonicated for 30 min prior to measurements the hydrodynamic diameters were 336±6 nm (polydispersity=0.164±0.0058), and 365±5 nm (polydispersity=0.162±0.0048) for food grade TiO$_2$ and gum TiO$_2$, respectively. These results suggest that many of the primary TiO$_2$ particles were aggregated together, although primary particles< 100 nm were clearly present.

Figure 2 shows the XRD spectra for food grade and gum TiO$_2$. Food grade and the gum TiO$_2$ consisted of anatase crystal structure only and not rutile or brookite, which have been found in some other food grade TiO$_2$ samples (Yang et al. 2014). For the gum TiO$_2$, there is a reflection not associated with anatase at 44.6° that is presumably from the 200 reflection from the aluminum

sample holder (theoretically at 44.8°). XRD spectra indicated that the lower bound of the food grade TiO$_2$ and gum TiO$_2$ size was 36 and 26 nm, respectively, which is in good agreement with the TEM results (i.e., Fig. 1).

Figure 3 shows the XPS spectrum for the O 1s spectral line for (a) food grade and (b) the gum TiO$_2$. For food grade TiO$_2$, the O 1s (532 eV) was shifted negatively, indicating O bonding on the surface. The large peak (2) was TiO$_2$ (530.1 eV) and the smaller peak (1) was presumably phosphate on the basis of the K 2p spectra (i.e., Electronic supplementary material (ESM), Supplemental Fig. 1) and the wide scan (i.e., ESM, Supplemental Fig. 2). For the K 2p spectra, the K 2$p_{3/2}$ line (294 eV) was shifted negatively to 293 eV, which is in agreement with referenced K$_3$PO$_4$ binding energies (Shih et al. 1998). For the wide scan, K is present and if it is assumed that the phosphate was in the form of K$_3$PO$_4$, then there would theoretically be an atomic

Fig. 2 XRD specta for food grade TiO$_2$ (*solid line*) and gum TiO$_2$ (*dashed line*) samples, plus standard reflections for anatase (*bottom*)
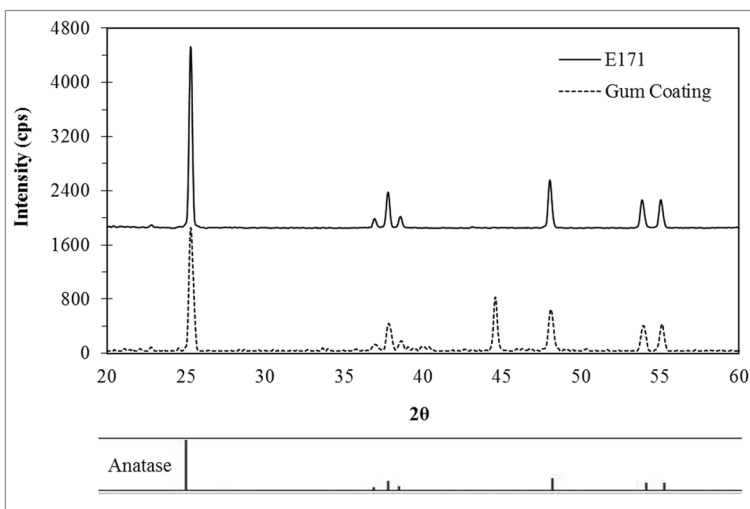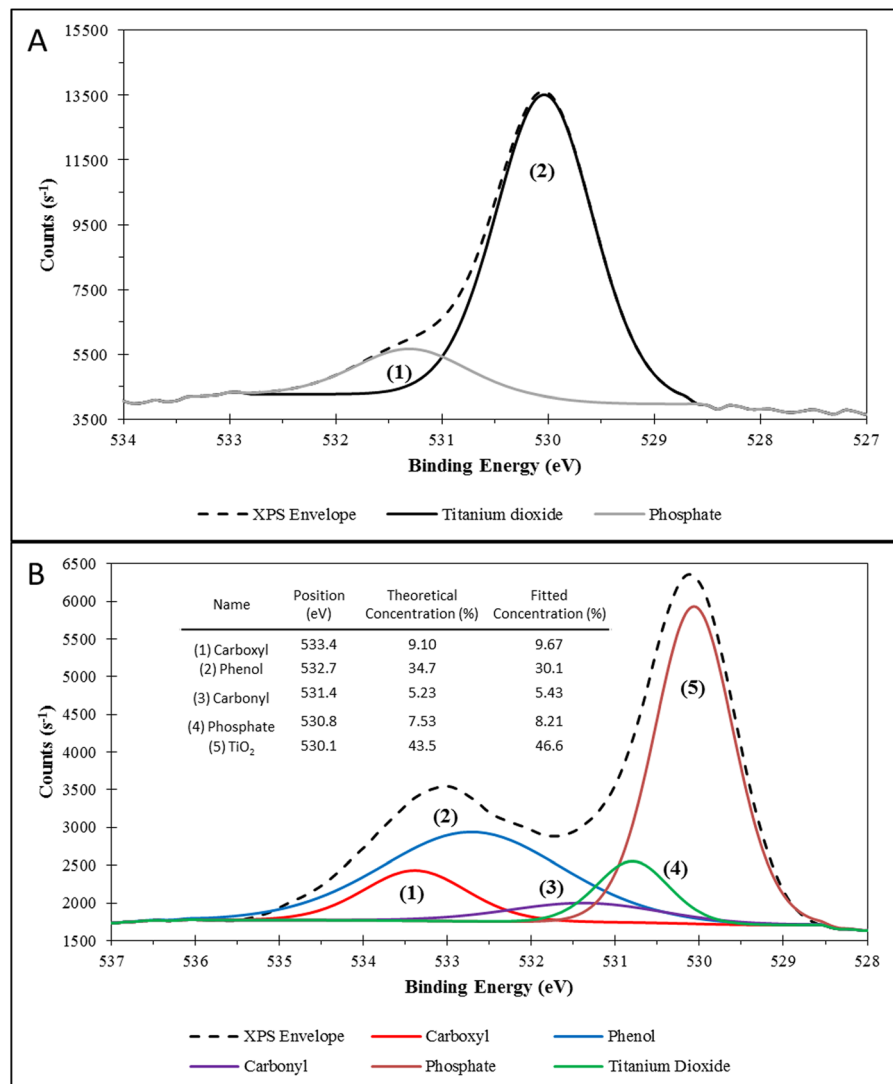
Fig. 3 XPS O 1s spectra of (**a**) food grade and (**b**) gum TiO$_2$. The inset table in (**b**) shows the theoretical atomic concentration taken from the XPS wide-scan (i.e., ESM, Supplemental Fig. 2) and calculated with the assumption of Ca$_3$(PO$_4$)$_2$ presence, and the fitted atomic concentration that is based on the O 1s XPS fittings shown in this figure (i.e., peaks 1, 2, 3, 4, and 5)

percentage of K of 9.6 %, which was in good agreement with the measured K amount of 10.8 %.

For the gum TiO$_2$, the O 1s was also shifted negatively, indicating bond formation. Similar to food grade TiO$_2$, there is a peak at 529.8 (peak 5) for TiO$_2$ and at 530.3 eV (peak 4), which was presumably a calcium phosphate compound on the basis of reference binding energies (Demri and Muster 1995) and the wide scan (i.e., ESM, Supplemental Fig. 3) that showed the presence of Ca. Assuming the compound was Ca$_3$(PO$_4$)$_2$, the theoretical atomic percentage of Ca would be 1.2 %, which was in good agreement with the measured value

of 1.8 % in the wide scan. Peak 1 at 533.4 eV, peak 2 at 532.7 eV, and peak 3 at 531.4 eV are carboxyl (COOH) (Weng et al. 1995), phenol (C-O) (Jouan et al. 1993), and carbonyl groups (C=O) (Gardner et al. 1995), respectively, as confirmed by referenced data and the C 1s spectra (ESM, Supplemental Fig. 4). The C 1s spectra has four peaks that correspond to (1) carboxyl (289.4 eV) (Clark and Thomas 1978), (2) carbonyl (288.1 eV) (Delpeux et al. 1998), (3) phenol (286.3 eV) (Delpeux et al. 1998), and (4) sp^2 C–C (284.8 eV) (Bachman and Vasile 1989). These bonds and their atomic ratios matched those found in the O 1s

spectra, thus confirming the identification of the surface contamination remaining on the TiO$_2$ gum coating.

In order to provide information on the surface charge characteristics of the TiO$_2$ samples, zeta potential analysis (Fig. 4) demonstrated that both the food grade TiO$_2$ and gum TiO$_2$ samples had a negative surface charge above pH=4. This was found to be a result of the phosphate and oxygenated functional groups found on the surface of the food grade TiO$_2$ and gum TiO$_2$, respectively. For the food grade TiO$_2$, the iso-electric point (IEP) pH was at approximately 3.3. The gum TiO$_2$ pH$_{IEP}$ was not observed at the pH range examined (~3–8.5), and at neutral pH, its zeta potential was significantly more negative (−46 mV) compared to the food grade TiO$_2$ (−19 mV).

Food grade TiO$_2$ disrupts the normal arrangement of constituent microvilli of the Caco-2$_{BBe1}$ brush border

Under optimal conditions differentiated Caco-2$_{BBe1}$ epithelia were shown to faithfully mimic the in vivo epithelium in the mucosal layer of the human enterocyte brush border (Peterson and Mooseker 1992, 1993; Peterson et al. 1993) when grown in cell culture. The organization of the brush border microvilli gives the apical surface of these cells an archetypical structure (Heintzelman and Mooseker 1992; Hirokawa et al. 1982; Mooseker 1985; Mukherjee and Staehelin 1971). Deviations from this archetypical structure can be easily detected in specimen exposed to experimental treatments when examined by scanning electron microscopy (SEM). This study exploits the archetypical structure of the brush border as an assay that is sensitive to changes in the normal organization of

the brush border. Food grade TiO$_2$ could be applied to this cell system to test if the brush border is disrupted.

In order to test if food grade TiO$_2$ disrupt the normal arrangement of microvilli, a SEM approach was employed. A representative, untreated Caco-2$_{BBe1}$ cell in a differentiated epithelium is viewed from above the apical cell surface (Fig. 5a). At this magnification (imaged at ×10,000), used in order to permit adequate detail, one cell occupied the field of view (Fig. 5a–d are shown at the same magnification). This region represents the surface that would face the lumen of the gut and had initial interaction with the TiO$_2$. At the ×10,000 magnification the structure observed are the tops of the many brush border microvilli. These microvilli stand straight off the surface of the cell, a condition referred to as erect ([De Beauregard et al. 1995] Fig. 5a) and had 43±7 microvilli/μm^2 (Fig. 5f). This number of microvilli in untreated specimens is so great that no relief (i.e., the plasma membrane between the bases of adjacent microvilli) can be seen. In contrast, gum TiO$_2$ (white arrows) appeared to decorate the surface of the epithelium and resulted in disruption of the brush border (Fig. 5b–d). Indeed, it was found that exposing Caco-2$_{BBe1}$ epithelia to 350 ng/mL (i.e., 100 ng/cm^2) of gum TiO$_2$ (white arrows) for 24 h produced brush borders whose constituent microvilli appeared limp and fewer in number (Fig. 5b). Quantification of the number of microvilli shown in Fig. 5b indicated that the brush borders contained 25±6 microvilli/μm^2 (n=9; Fig. 5f). Exposure to 3.5 μg/mL (i.e., 1 μg/cm^2) of gum TiO$_2$ (white arrows) more clearly illustrated the limpness of the microvilli (Fig. 5c). These microvilli appeared to rest on one another to bolster the standing morphology of the microvilli (Fig. 5c). Quantification of the microvilli after

Fig. 4 Zeta potential analysis for food grade TiO$_2$ and gum TiO$_2$. TiO$_2$ samples were measured with respect to pH. Both food grade TiO$_2$ and gum TiO$_2$ have negative zeta potentials. Note that the zeta potential of food grade TiO$_2$ is less negative and consequently agglomerates faster in solution compared to the gum TiO$_2$ samples employed in this investigation
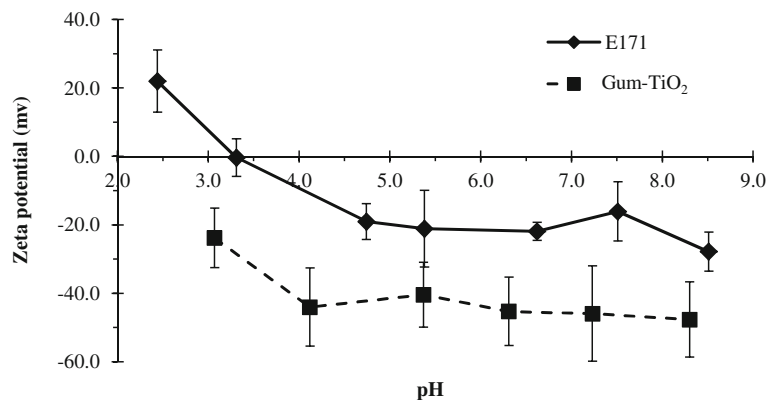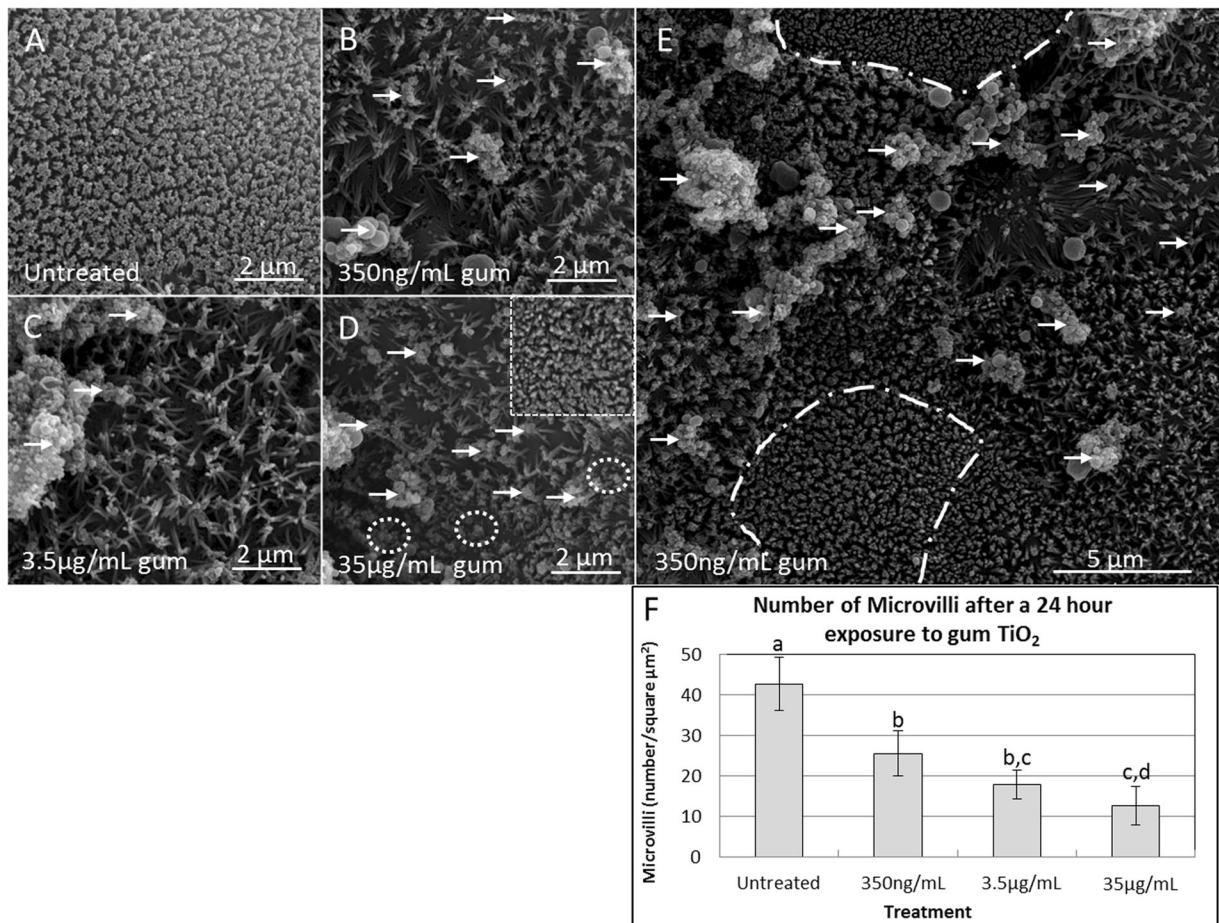
Fig. 5 Exposure to food grade TiO_2 isolated from name-brand gum resulted in disruption of the brush border as evidenced by SEM. **a** Untreated, control specimens appeared well-organized and densely packed with many brush border microvilli. **b** Exposure to 350 ng/mL gum TiO_2 for 24 h reduced the number of standing microvilli. The *white arrows* point to the TiO_2. **c** Exposure to 3.5 µg/mL gum TiO_2 for 24 h apparently caused the microvilli to go limp. **d** Exposure to 35 µg/mL gum TiO_2 for 24 h resulted in brush border microvilli that appeared retracted, and contained almost no erect microvilli. The *inset* in **d** is a control specimen, whereby the TiO_2 was applied to complete culture medium at a concentration of 35 µg/mL, the TiO_2 was allowed to settle, and the top fraction was used to feed the epithelia. This control specimen appeared identical to the untreated control. (**e**)

The low magnification micrograph showed that the effect of exposure to 350 ng/mL gum TiO_2 for 24 h was localized to those cells that were in intimate contact with the TiO_2. Some regions within the micrograph showed signs of microvilli that may have been depressed by TiO_2. The alternating *dashed line* surrounds cells that had no material on the cell surface and consequently a developed brush border. The *white arrows* point to gum TiO_2. (**f**) The histogram shows the number of microvilli after the dose response experiment. The data is shown as mean±SEM, and significance ($p<0.05$) was determined based on a one-way ANOVA followed by Dunn's posttest. Characters represent significance where redundant characters indicate non-statistical differences

exposure to this concentration indicated that the brush borders had 18 ± 4 microvilli/µm^2 ($n=9$; $p<0.001$; Fig. 5f). Exposure to 3.5 µg/mL (i.e., 10 µg/cm^2) of gum TiO_2 (white arrows) demonstrated brush borders whose apical surface appeared absent of microvilli in some regions, and whose apical membrane appeared decorated with membrane "blebs" (dotted white circles) of approximately 100 nm in diameter (Fig. 5d). Quantification of the number of microvilli shown in

Fig. 5d indicated that the brush borders contained 12 ± 5 microvilli/µm^2 ($n=9$; $p<0.001$; Fig. 5f).

It is important to rule out the possibility that leeching of ions from the food grade or gum materials, or sequestration of serum components by the TiO_2, resulted in disruption of the brush border. In order to test this, gum TiO_2 at a concentration of 35 µg/mL (i.e., 10 µg/cm^2) was applied to culture medium, the medium was sonicated, and the TiO_2 were allowed to settle through

sedimentation to the bottom of a conical tube. Once the TiO_2 settled as evidenced by visual inspection the culture medium, the top 1/3 of the supernatant was employed as growth medium for epithelia and the following day the specimens were cytologically fixed and processed for SEM. Through the use of single particle ICP-MS, it was found that approximately 99.99 % titanium settled, while 0.01 % remained in the supernatant, and when this medium was applied to the epithelium (shown as the inset in Fig. 5d), SEM analysis indicated that the brush borders appeared well ordered and densely packed identical to untreated control microvilli. Of note, the effect of the 350 ng/mL (i.e., 100 ng/cm^2) of gum TiO_2 (white arrows) appeared to be a localized effect (Fig. 5e). Only those areas that were found to be in intimate contact with the agglomerated NPs (white arrows) showed regions devoid of microvilli (imaged at ×4,300 in Fig. 5e). Regions devoid of the TiO_2 (outlined by the alternating dashed lines) had an erect, dense array of microvilli on the apical surface of the cell whereas regions with gum TiO_2 had limp and fewer microvilli surrounding the gum TiO_2. The regions in Fig. 5 pointed to by white arrows are presumed to be agglomerated gum TiO_2 as SEM coupled with energy dispersive x-ray spectroscopy showed round, electron-dense aggregated material (Fig. 6a) with identifying peaks corresponding to titanium and oxygen (Fig. 6b). Analysis of particle diameters indicates that some TiO_2 were NPs as the smallest particle measured was 20 nm whereas the largest was 291 nm in diameter after sputter coating.

In light of the fact that the food grade and gum TiO_2 are of the same crystal structure (anatase), and food grade TiO_2 (E171 compliant) is a pigment for use in human foods, one might predict that exposure to food grade TiO_2 results in a similar disruption of the Caco-2$_{BBe1}$ brush border. In order to test this possibility, a dose–response experiment was conducted. Consistent with the results of Figs. 5 and 7, it indicates effacement of the brush border after the 24-h exposure window. It was found that untreated specimens had microvilli that appeared erect (Fig. 7a) with 43±7 microvilli/μm^2 (Fig. 7f). Similar to the results reported in Fig. 5, exposure to 350 ng/mL (i.e., 100 ng/cm^2) of food grade TiO_2 (white arrows) resulted in a slightly limp microvillar morphology (Fig. 7b) and brush borders contained 26±5 microvilli/μm^2 (Fig. 7f). Exposure to 3.5 μg/mL (i.e., 1 μg/cm^2) of E171 TiO_2 (white arrows) produced brush border with individual microvilli apparently limp (Fig. 7c), and quantification of the number of microvilli

indicated that there were 21±7 microvilli/μm^2 (Fig. 7f). After exposure to 35 μg/mL (i.e., 10 μg/cm^2) of food grade TiO_2 (white arrows) microvilli appear tethered at the plus tips and laying perpendicular to the plasma membrane. This disrupted phenotype was prevented by permitting sedimentation of the food grade TiO_2 to occur in vitro and subsequently culturing epithelia in the supernatant largely removed of the TiO_2 (inset in Fig. 7d) as was done early with the gum TiO_2. Finally, incubating 350 ng/mL (i.e., 100 ng/cm^2) of food grade TiO_2 (white arrows) appeared only to locally affect the normal arrangement of the microvilli (originally imaged at ×4,300), as those cells with agglomerated colloids at the cell surface showed a mildly limp/clustered morphology (Fig. 7e).

Agglomerated TiO_2 do not remain stationary at the surface of the epithelium

The presence of agglomerated TiO_2 on the cell surface presents the possibility of a direct interaction between the agglomerates and the brush border. In order to determine if there is a direct interaction between the agglomerates and the brush border, a time-lapsed video microscopy approach was employed. This was possible because the agglomerated colloids were within the limit of resolution of light microscopy , but a large subset of the material maintained at least one or more external dimension< 100 nm in diameter as a characteristic of a NP (Dunphy Guzman et al. 2006). When viewed with phase-contrast microscopy, untreated specimens showed a typical honeycomb arrangement of cells within the epithelium (Fig. 8a, Supplemental Video 1). Upon careful inspection of those epithelia exposed to 3.5 μg/mL (i.e., 1 μg/cm^2) food grade TiO_2, there appeared to be phase-dense, granular material at the cell surface. More importantly, Fig. 8b showed agglomerates (white arrows) decorated the apical surface of the epithelium and these agglomerates apparently moved position with respect to time (Fig. 8b, Supplemental Video 2); The black rectangle in Fig. 8b surrounds one such agglomerate collected as four still frames every 10 s. The white arrow head points to the TiO_2 agglomerate midpoint, and a white line was inscribed from the midpoint of the arrowhead to the fixed end of the micrograph. Under these conditions, the length of the fixed end of the micrograph to the midpoint of the arrowhead changed (shown in arbitrary units *; the scale bar is 20 μ in A–B) indicating movement of the putative TiO_2 agglomerates.
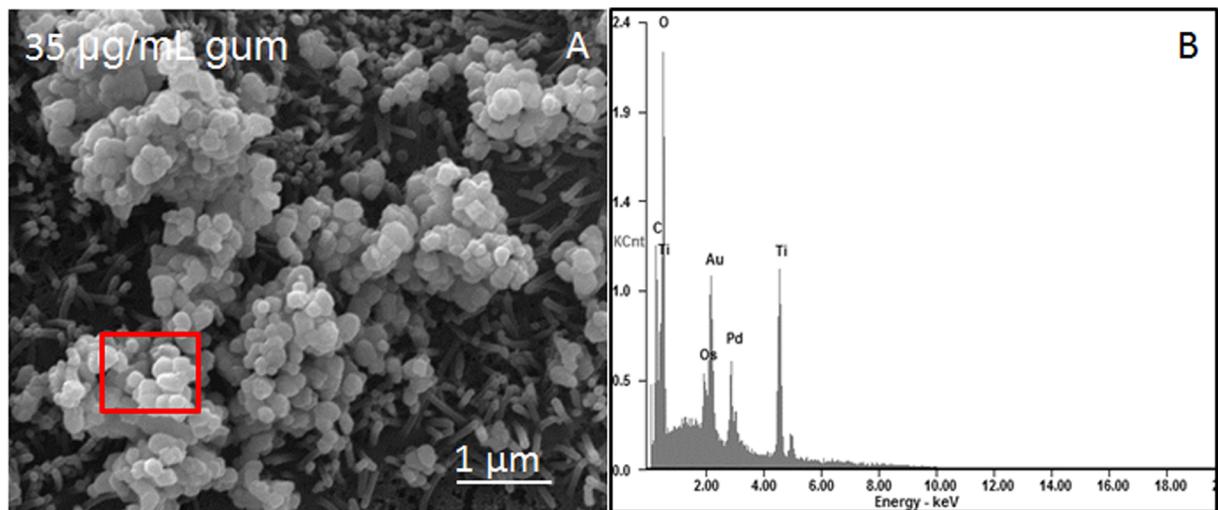
Fig. 6 The material on the surface of the epithelia was TiO_2 as determined by EDX analysis. **a** The micrograph shows a high magnification view of the material that decorated the epithelia. The morphology of the material appears similar to the TEM micrographs shown in Fig. 1. The *red box* is the region of interest for EDX analysis. **b** EDX analysis indicated that the material was composed of titanium and oxygen. The osmium peak was apparently due to the secondary fixative (OsO_4) used for the underlying biological specimens (i.e., the brush border), and the Pd/Au was the material used to sputter coat the specimens

In order to assess if these phase-dense, granular material might be the TiO_2 agglomerates the TiO_2 was applied to a glass bottom dish at 3.5 µg/mL (i.e., 1 µg/cm^2) in the presence of cell culture medium, but devoid of cells. This positive control for the agglomerated TiO_2 demonstrated phase-dense, granular material moving at the bottom of the culture dish. The white oval in Fig. 8c showed that the position of the agglomerated TiO_2 changed with time. Furthermore, and similar to the result described in Fig. 8b, the measuring device indicated that the length of the inscribed white line changed over time (Fig. 8c, Supplemental Video 3; shown in arbitrary units *; the scale bar in the still frames is 8 µm). The same region shown in Fig. 8c was washed to remove any unbound TiO_2 and a correlated light and SEM approach was employed in order to show the material in high magnification, as well as to conduct elemental analysis (Fig. 8d). From left to right, the first micrograph indicated that some TiO_2 adhered to the collagen after washing the dish three times with deionized water. The white arrow in each image points to the top portion of the "L" that was employed as a feducial marker. The second image showed that the specimen remained largely unchanged after processing the slide for SEM. The third image is a higher magnification of the top portion of the "L" (white arrow). The fourth image showed a high magnification view of the top of the "L" etched in the glass. The white dashed box was

the region used to determine elemental composition (data not shown). It was found that this region contained peaks corresponding to titanium and oxygen as expected for TiO_2. What follows from these results is that after sedimentation the agglomerated TiO_2 moved, potentially through Brownian motion (Cho et al. 2011). Coupled the effects of sedimentation and movement might depress the microvilli and permit adsorption/effacement of the brush border.

Disruption of the brush border is independent of sedimentation due to gravity

The clue that agglomerated TiO_2 oscillated on the surface of the epithelium and that food grade TiO_2 results in disruption of the brush border suggested that sedimentation due to gravity and consequently the mass of the agglomerated TiO_2 may account for brush border disruption. In order to test this prediction, two alternative approaches to remove the effects of gravity and consequently the mass of the nanomaterial were employed; first by inverting the configuration of the epithelia during exposure to TiO_2 illustrated in the cartoon, and second by culturing the epithelia in a microgravity bioreactor (Fig. 9a–b). During inverted culture of untreated Caco-2$_{BBe1}$ epithelia, the morphology and density of the microvilli was not found to be different than untreated specimens in the upright configuration (Fig. 10a).
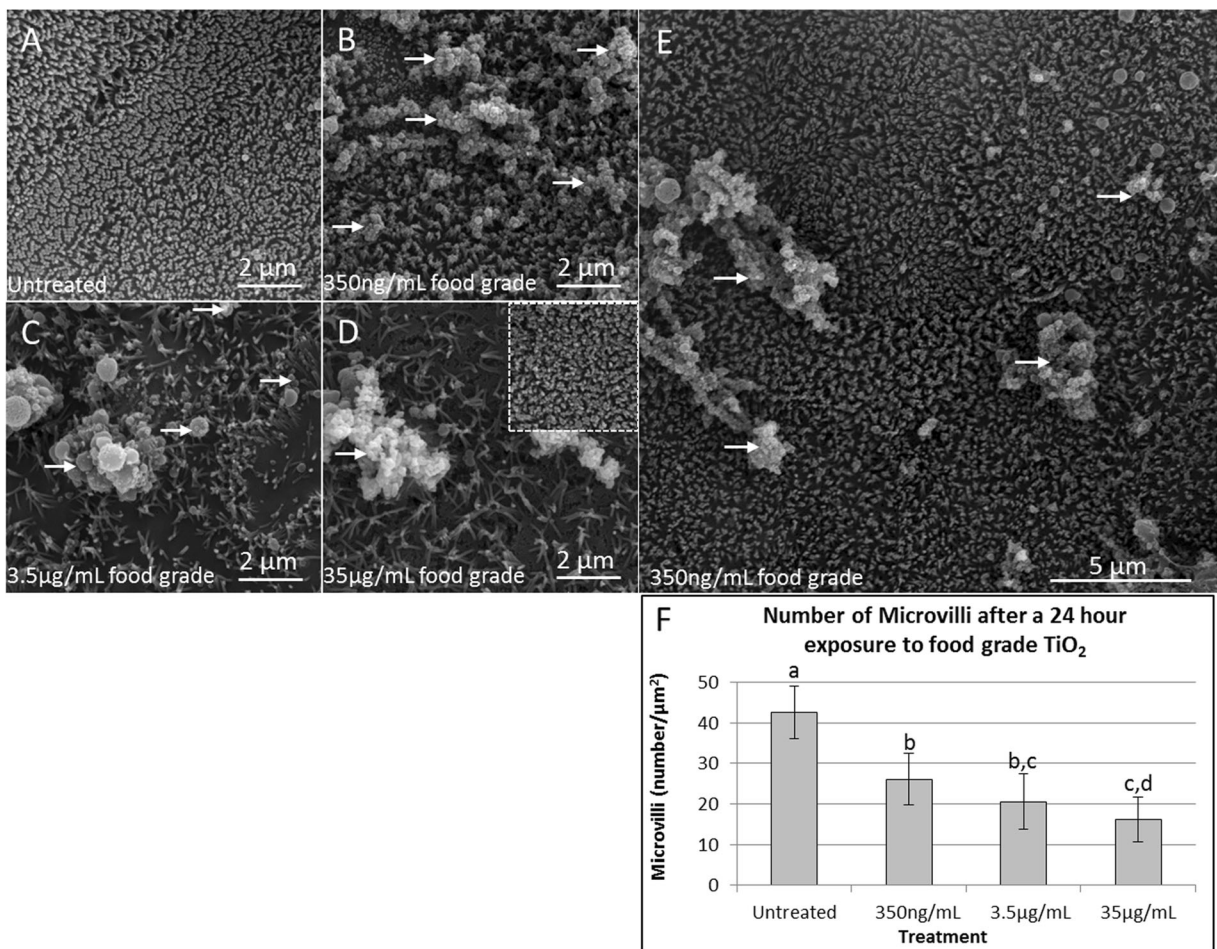
Fig. 7 SEM analysis indicates that food grade (E171 compliant) TiO$_2$ disrupted the brush border microvilli. **a** Untreated, control specimens retained a well-developed brush border after sustained culture. Note that at least two edges of individual cells can be seen as identified by the slight interdigitation of microvilli between adjacent cells. **b** Exposure to 350 ng/mL food grade TiO$_2$ for 24 h reduced the number of standing microvilli. The *white arrows* point to the TiO$_2$. **c** Exposure to 3.5 μg/mL food grade TiO$_2$ for 24 h apparently caused the microvilli to go limp. The *white arrows* point to the TiO$_2$. **d** Exposure to 35 μg/mL food grade TiO$_2$ for 24 h resulted in brush border microvilli that appeared limp/disorganized, and the plasma membrane of the cell was easily seen indicating a significant loss of microvilli. The *arrows* point to the TiO$_2$. The inset in D is a control specimen, whereby the TiO$_2$

was applied to complete culture medium at a concentration of 35 μg/mL, the TiO$_2$ was allowed to settle, and the top fraction was used to feed the epithelia. This control specimen appeared identical to the untreated control. **e** The low magnification micrograph showed that the effect of exposure to 350 ng/mL food grade TiO$_2$ for 24 h was localized to those cells that were in intimate contact with the TiO$_2$. The *white arrows* point to the TiO$_2$. **f** The histogram shows the number of microvilli after the food grade TiO$_2$ dose response experiment. The data is shown as mean± SEM. Significance ($p < 0.05$) was determined by a one-way ANOVA followed by Tukey posttest. Characters represent significance where redundant characters indicate non-statistical differences

However, exposure to 350 ng/mL (i.e., 100 ng/cm^2) of food grade TiO$_2$ (white arrows) while the epithelium was in the inverted configuration appeared to disrupt both the erect morphology of the microvilli and the total number of microvilli; SEM analysis indicated that the microvilli were limp (Fig. 10b) and quantification of the number of microvilli indicated that there was a significant reduction to a value of 23±6 microvilli/μm^2.

Furthermore, the brush border effacement was confirmed during inverted exposure to food grade TiO$_2$ at a concentration of 350 ng/mL (i.e., 100 ng/cm^2; Fig. 10c, d). That is, the microvilli appeared limp in regions decorated with agglomerated TiO$_2$ (white arrows), and the number of the microvilli was significantly reduced to 27±8 microvilli/μm^2. The black arrows point to TiO$_2$ settled at the inverted bottom of the
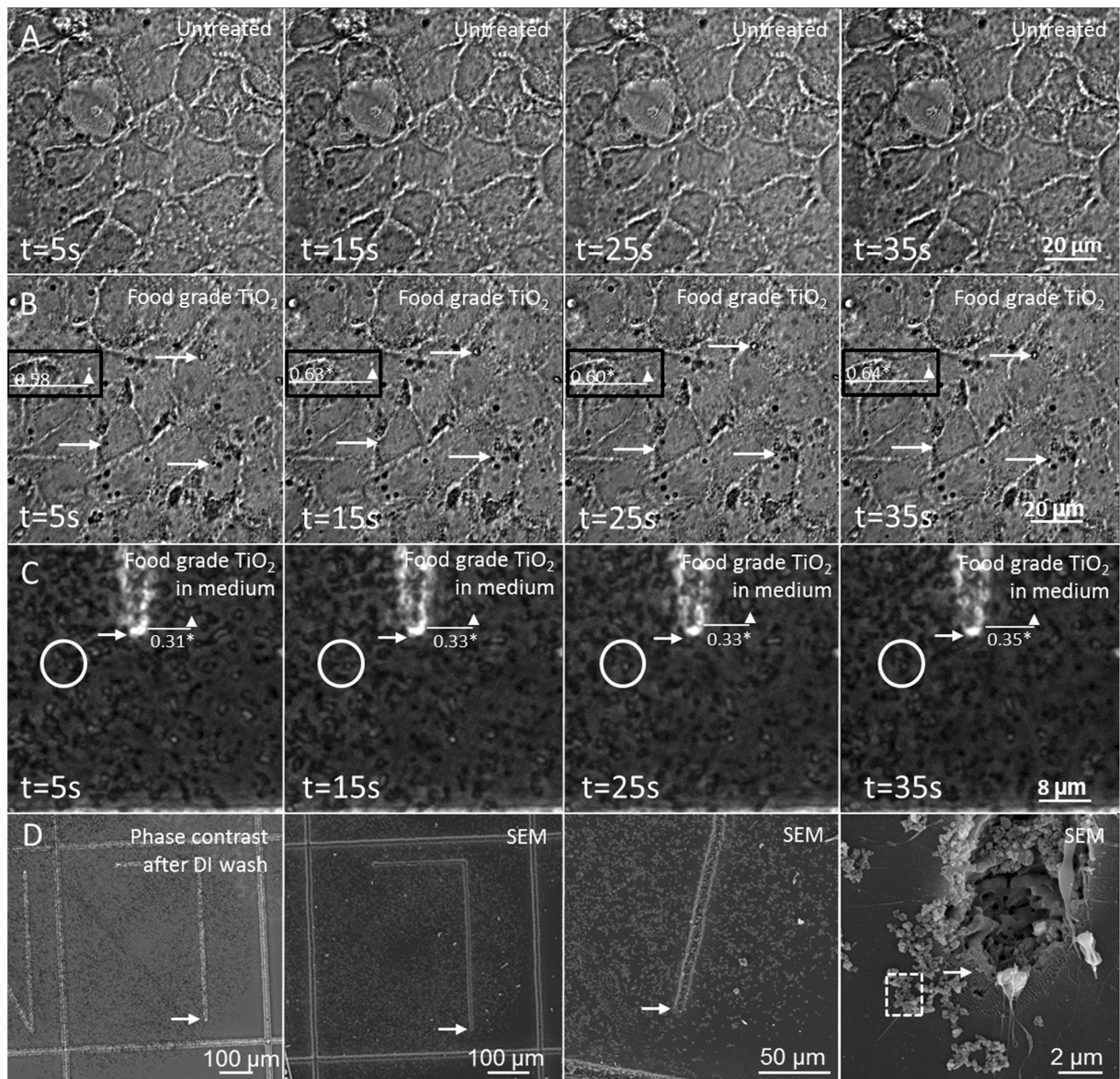
Fig. 8 Live cell imaging indicates that agglomerated TiO$_2$ settles and moves with respect to time. **a** Untreated, control specimens show the typical honeycomb arrangement of phase-light junctions between cells. No granular material is evident in the complete culture medium, or at the cell surface. **b** Application of 3.5 μg/mL food grade TiO$_2$ resulted in granular material, pointed to by *white arrows*, that appeared to oscillate on the surface of the epithelia. The *red circle* shows one such event; the center of the putative TiO$_2$ agglomerate changed position over time indicated by a change in arbitrary units from a fixed point at the edge of the micrograph. **c** Applying food grade TiO$_2$ to a gridded Ibidi dish in the absence of cells indicated that the granular material shown in B was

agglomerated TiO$_2$. **d** The data shown in C were confirmed to be TiO$_2$ through the use of SEM coupled with EDX analysis. From *left to right*, the top of the "L" (*white arrow*) was employed as a feducial marker. The first image corresponds to the TiO$_2$ that adhered to the collagen after washing with deionized water to remove salts. The second image is the same "L," but imaged with a SEM. The third image is a higher magnification of the second. The fourth image is further magnified and shows agglomerated TiO$_2$. The *white arrow* in each micrograph of C and D points to the top portion of the "L." The *red dashed box* is the region of interested employed for EDX analysis. EDX indicated that these regions contained peaks corresponding to titanium and oxygen

centrifuge tube (Fig. 9b). No statistical difference in the number of microvilli was found after exposure to neither gum TiO$_2$ nor food grade TiO$_2$ at any concentration or

epithelial orientation. These data were confirmed employing the microgravity bioreactor (Fig. 9c). The white arrow in Fig. 9c points to the cell monolayer in
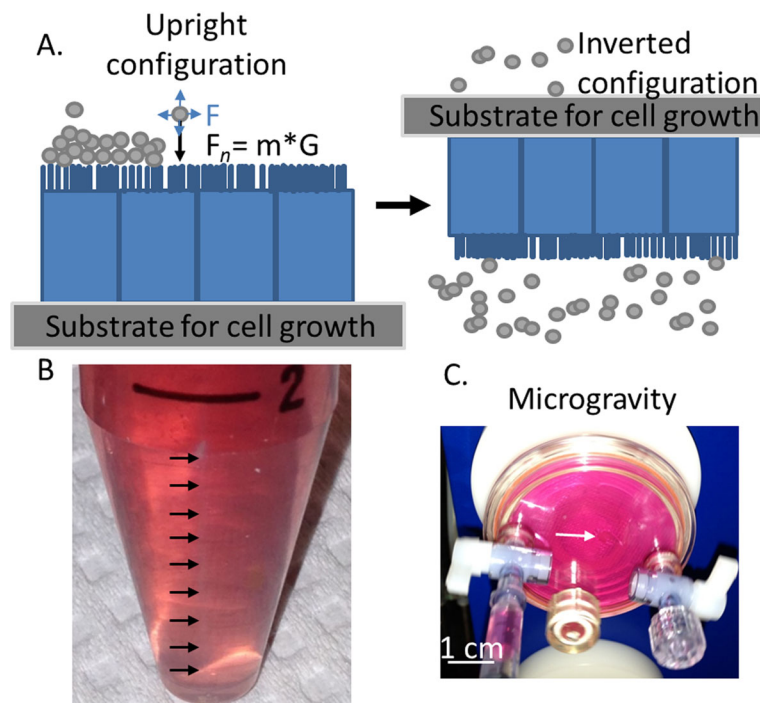
Fig. 9 The cartoon and images illustrate the experimental design to remove the effects of sedimentation. **a** During exposure to TiO$_2$ in the upright condition could permit sedimentation of the TiO$_2$. However, an alternative scenario exists whereby the epithelia are inverted and the TiO$_2$ can no longer settle at the cell surface. **b** After culturing epithelia in the inverted position a thin, white line appeared at the bottom of the tube that housed the specimens. The *arrows* point to the TiO$_2$ that settled. **c** The microgravity bioreactor permitted conditions of microgravity thereby eliminating settling of the TiO$_2$. The *white arrow* points to an epithelium whose collagen-coated, PTFE membrane was excised from the plastic housing. The central position of the substrate containing the epithelium indicates that it is in a state of microgravity

microgravity at the center of the culture disk and this is the proper location for the cells to be exposed to microgravity (Schwarz and Wolf 1991).

Food grade TiO$_2$ is internalized by cells of the Caco2$_{BBe1}$ human intestinal model

Several lines of evidence indicate that internalization of NPs could play a role in actin remodeling at the apical surface of the cell (Faust et al. 2014b; Kalive et al. 2012; Zhang et al. 2010; Koeneman et al. 2010). Remodeling of the actin cytoskeleton at the apical surface (i.e., the brush border) could result in disruption of the brush border, since microvilli would not exist if remodeling occurred. In order to test if food grade TiO$_2$ was internalized by the Caco-2$_{BBe1}$ epithelia, a TEM approach was employed. Under optimal conditions the brush border of differentiated Caco-2$_{BBe1}$ epithelia demonstrated polarity with numerous brush border microvilli at the apical surface as an untreated control (Fig. 11a). After a 24-h treatment with either 350 ng/mL (i.e., 100 ng/cm^2)

of gum TiO$_2$ or 350 ng/mL food grade TiO$_2$ (black arrows) two populations of nanomaterial existed (Fig. 11b–d). There was a subset of agglomerated TiO$_2$ enclosed by electron dense vesicles as internalized material, and another fraction remained in an electron-dense granular material "tangled" in the brush border at the cellular apex (Fig. 11b–d). Analysis of the individual particle diameters within each of the micrographs indicated a range of sizes from as small as 58 nm to as large as 286 nm, indicating that a subset of the internalized particles were NPs.

Discussion

In the present investigation, it was found that food grade TiO$_2$ disrupted the brush border after exposure to an in vitro model of the human intestine. A significant fraction of this food grade TiO$_2$ had dimensions of primary particles<100 nm in its longest-axis length. Specifically, we addressed the hypothesis that exposure
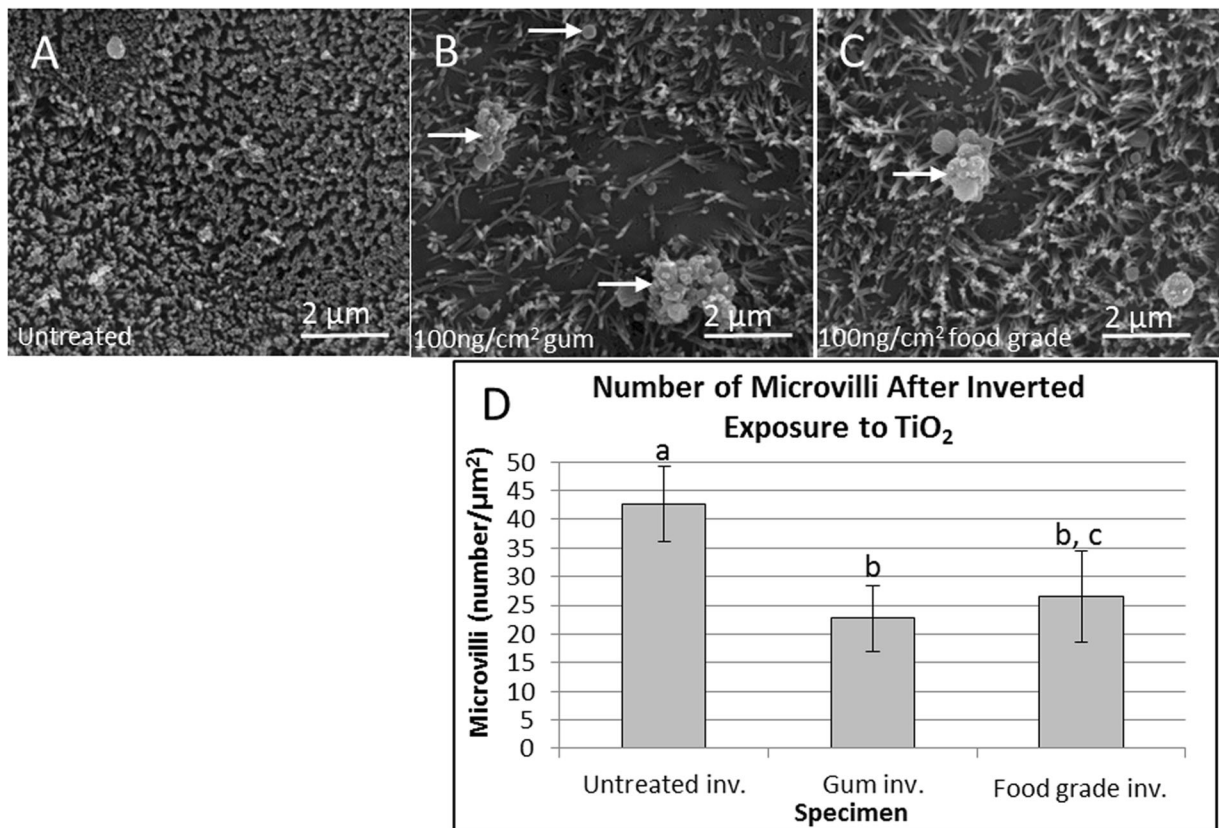
Fig. 10 Inverting the specimens to remove the effects of TiO_2 settling indicate that sedimentation does not account for brush border disruption. **a** Untreated specimens, when grown upside-down retain a well developed and densely packed brush border. **b** Exposing the specimens to a concentration of 350 ng/mL gum TiO_2 while inverted resulted in disruption similar to that found during right side up culture. The *white arrows* point to gum TiO_2. **c** Exposing the specimens to a concentration of 350 ng/mL food grade TiO_2 while inverted resulted in disruption similar to that found during upright culture. The *white arrows* point to gum TiO_2. **d** The histogram indicates that there is a significant reduction in the number of microvilli between untreated, and TiO_2 treated specimens. No statistical difference was observed between inverted and upright exposure to TiO_2. Characters represent significance where redundant characters indicate non-statistical differences

to food grade TiO_2 results in brush border disruption and disruption due to TiO_2 is an event independent of sedimentation in vitro. The study by Cho et al. indicated that large and/or dense metal NPs have the potential to rest on top of the cells at the bottom of the culture dish, which could be due to the effects of NP agglomeration and subsequently sedimentation. This settling out of solution after agglomeration could increase the concentration of NPs that the epithelium would otherwise not be exposed to. In the present investigation it was found that TiO_2 purchased as food grade (E171 coded) as well as TiO_2 isolated from the candy coating of gum were of similar physico-chemical characteristics. These particles exposed to the epithelia at the lowest concentration of 350 ng/mL (i.e., 100 ng/cm^2) that elicited a cellular response when grown upright, also resulted in brush

border disruption after removing the effects of TiO_2 settling due to sedimentation. This effect was first demonstrated when the substrate with the epithelium was inverted and exposed to TiO_2 at a concentration of 350 ng/mL. Under these conditions, there was no statistical difference between those exposed to TiO_2 in neither the upright nor the inverted configurations. This result was confirmed by an independent approach where epithelia were exposed to TiO_2 under conditions of microgravity, indicating that sedimentation of agglomerated TiO_2 does not account for disruption of the brush border. Furthermore, results from control experiments indicate that it is unlikely that leeching of ions, or adsorption of serum components from/to TiO_2 resulted in brush border disruption as exposure to cell culture medium removed of the TiO_2 resulted in brush borders that
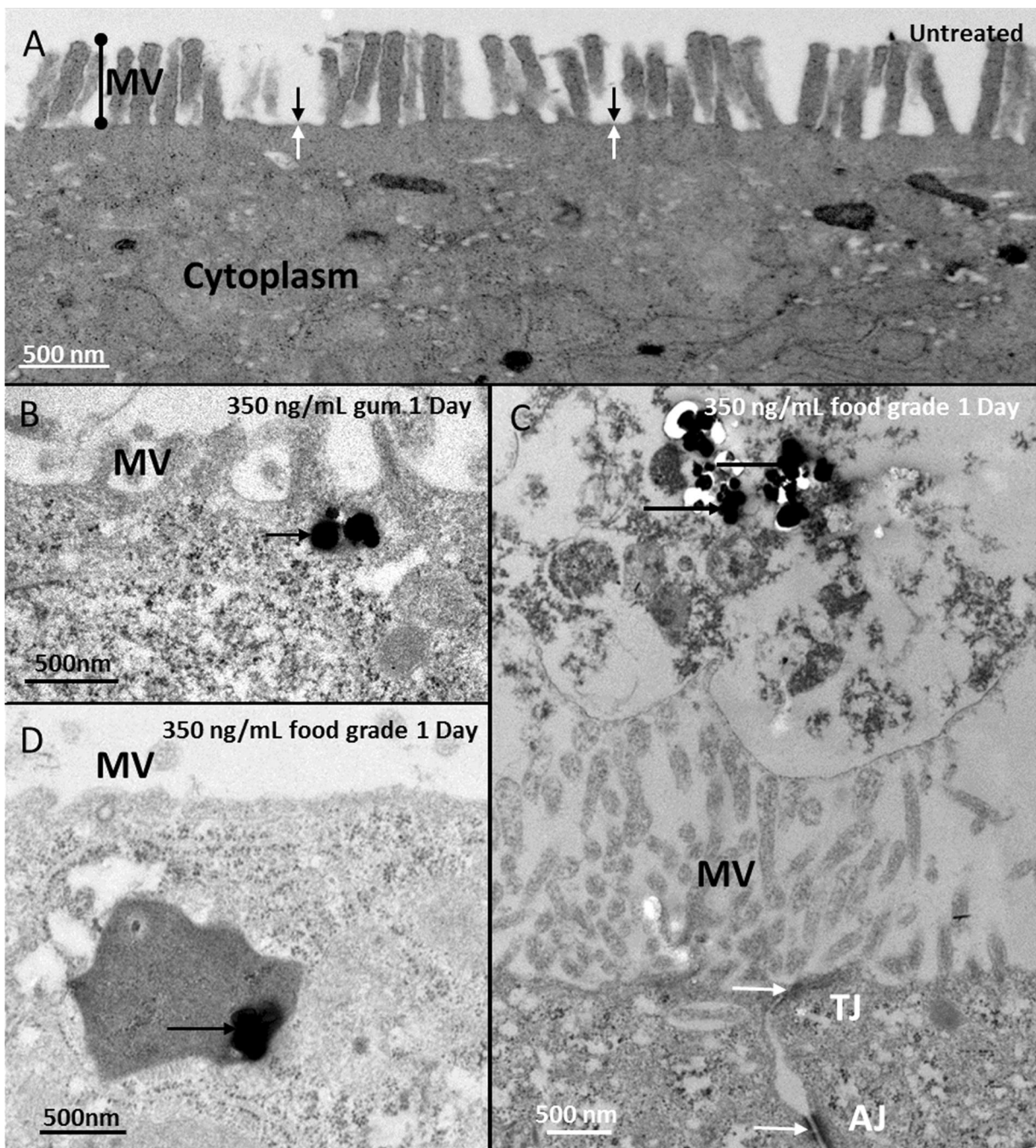
Fig. 11 TEM analysis indicates that the TiO_2 was internalized as early as 1 day after exposure to 350 ng/mL of TiO_2. **a** Untreated, control specimens showed apical differentiations (i.e., brush borders), an electron-dense terminal web region, and an organelle-free zone. The microvilli appear numerous and well-ordered. The black and *white arrows* point to the plasma membrane of the cell. **b** Exposure to 350 ng/mL gum TiO_2 after 1 day resulted in internalization of the TiO_2, and limp microvilli. The *black arrow* points to

the electron-dense TiO_2. **c** Exposure to 350 ng/mL food grade TiO_2 after 1 day resulted in a subset of TiO_2 found enmeshed within an amorphous network at the tops of some cells. The microvilli were disorganized. However, tight- and adherens junctions were seen (pointed to by the *white arrows*). (**d**) Exposure to 350 ng/mL food grade TiO_2 after 1 day also showed that the TiO_2 was internalized. The *black arrow* points to the TiO_2

appeared healthy and morphologically similar to unexposed (control) brush borders.

Studies have shown that exposure to α-Fe_2O_3 NPs at a concentration of 100 μg/mL elicited an upregulation of the gene (*CapZ*) that encoded the actin capping protein CapZ in the Caco-2 cell model (Kalive et al. 2012) and in a brush border expressing model of the human placenta (Faust et al. 2014b). As indicated in the Introduction, it is well known that elongation of filamentous actin (F-actin) coupled with the addition of actin bundling proteins to the core fine filaments permits the normal morphology of the microvillus. Studies have also shown that polymerization of actin occurs at the most distal point of the microvillus tip in a region referred to as plus tips (Ishikawa et al. 1969; Tilney and Mooseker 1971; Begg et al. 1978; Hirokawa and Heuser 1981). Further, the addition of actin monomers to F-actin is known to be a dynamic and continuous process (Stidwill et al. 1984). In the event that the actin capping protein, CapZ is translated from upregulated messenger RNA, CapZ could inhibit F-actin polymerization at the plus tips. This hypothesis is corroborated by the constant turnover of the structural proteins, and addition of monomers at the plus tips; should CapZ protein cap F-actin plus tips, there would be no regulated addition of monomers necessary to maintain the microvilli length.

In vitro analysis necessitates the use of a physiological milieu containing serum proteins. Commonly, investigators use serum at a 10 % concentration in a liquid medium formulated with the necessary salts, vitamins, minerals, etc., as a surrogate for a chemically defined culture medium in order to propagate cells in a culture dish. When materials such as metal nanoparticles are applied to this medium, the proteins from the medium adsorb to the material surface. Since some nanoparticles have a large surface-area-to-volume ratio and consequently high surface free-energy, a large number of proteins have been shown to decorate the material surface based on material surface chemistry (Lundqvist et al. 2008). These decorated proteins bind with different affinities and are referred to as the "hard" and "soft" coronas (Milani et al. 2012). Studies employing non-functionalized (i.e., pristine) silica nanoparticles clearly showed the effects of the NP corona (Lesniak et al. 2012). In the study by Lesniak and coworkers, pristine silica nanoparticles (50 nm in diameter) were exposed to A549 lung epithelia in serum-free conditions for 1 h and were found decorated with a variety of proteins after recovery of the nanomaterial from the cells. Of note, the proteins spectrin and α-actinin had high spectral counts during mass spectrometry analysis, indicating a large number of these proteins were part of the NP corona (Lesniak et al. 2012). Although purely speculative, one could hypothesize that a similar process may result in brush border disruption as was shown to be independent of sedimentation in the present investigation. Both spectrin and α-actinin are necessary for the structural integrity of the terminal web and inter-microvillar rootlets. If spectrin and α-actinin adsorbed to the NP corona with a higher affinity than serum components and/or the proteins that directly bind spectrin and α-actinin in the terminal web, it could be predicted that particles, such as the TiO_2 employed in the present investigation, sequester these structural components. Sequestration of structural proteins necessary to maintain the erect morphology of microvilli could transiently disrupt the brush border since, as indicated in the preceding paragraph, many of the proteins in the microvilli are constantly turned over, and retrograde actin flux coupled with monomer addition at the plus tips maintains the length of microvilli in a highly controlled manner. Therefore, at present, the possibility that the biological corona is in part responsible for brush border disruption cannot be excluded from the putative list of causal agents.

To date, a number of studies using TiO_2 NPs have been conducted in order to determine whole organism (in vivo) toxicity as a result of exposure to TiO_2 and not the "subtle" effect of brush border disruption as a consequence of exposure to TiO_2 from human food products as was found in the present investigation. Studies conducted in the mouse model indicate a wide range of effects after intragastric administration of anatase TiO_2 NPs (Duan et al. 2010). The authors, employing concentrations of 0, 62.5, 125, and 250 mg/kg body weight every other day, found significant loss in body weight at concentrations of 125 and 250 mg/kg TiO_2 NPs exposure (Duan et al. 2010). One possible explanation for the significant loss of body weight between control groups and those exposed to 125 and 250 mg/kg body weight of anatase TiO_2 NPs is a disruption manifested as a retraction of the brush border. If brush borders were disrupted in this system, there would be a net loss of surface area by which food stuffs could be absorbed. The decrease in surface area of the small intestine could result in malnutrition and decreased body weight. However, when mice were dosed once by oral gavage according to the OECD protocol, acute toxicity was observed and resulted in an increase in body weight (Wang et al. 2007).

Further, studies employing the rat model indicate no change in body weight. In the study (Warheit et al. 2007), the authors applied 175, 550, and 1,750 mg/kg of ultrafine mixtures of TiO$_2$ NPs (79 % rutile 21 % anatase) once to a single fasted female ($n=1$) and investigated the effects 14 days after dosing according to the OECD protocol (Oecd 1994). Of note the authors dosed three rats as a single experiment at concentrations of 5 g/kg body weight with the same material and found no change in body weight after 14 days (Warheit et al. 2007). However, many of the in vivo studies have not directly addressed the "subtle," non-lethal phenomenon of brush border disruption. Therefore, at present there is evidence for and against in vivo brush border disruption, which appear to be dose and species dependent.

There are several in vivo studies indicating that TiO$_2$ can translocate to the liver, kidney, and brain in rodents (Duan et al. 2010; Fröhlich and Roblegg 2012; Hu et al. 2010; Powell et al. 2010; Wang et al. 2007). This fact implies that TiO$_2$ was able to pass several of the physiological barriers that could otherwise sequester the material from direct interaction with the epithelium. Perhaps the greatest physiological barrier that exists in mammals including rodents, but not the in vitro cell model employed in the present investigation, is mucus. Mucus is secreted by goblet cells that are interspersed within the in vivo mucosal layer. Of their many functions, goblet cells largely serve to lubricate and "protect" the enterocytes/brush borders from abrasion. Furthermore, it is widely accepted that the entire mucosal layer is turned over every 4–5 days in mammals including rodents (van der Flier and Clevers 2009). Therefore, if brush border disruption occurred in these systems, evidence for this event would be found shortly after administration of the TiO$_2$ and is liable to present itself as a retraction/shortening of the microvilli. Disruption of the brush border in vivo could appear as a retraction for a number of reasons. In an attempt to investigate proteins necessary to maintain the archetypical structure of the microvillus, investigators have developed several knockout models for a number of structurally important brush border proteins in rodents (Ferrary et al. 1999; Grimm-Günter et al. 2009). In spite of triple knockdown models, microvilli still appeared on the apical cell surface (Revenu et al. 2012). These data potentially indicate that there is functional redundancy within the in vivo system in rodents to maintain the erect microvilli morphology that may not exist in the Caco-2$_{BBe1}$ human cell model since this cell system appears

amenable to experimental manipulations that result in changes in the brush border (De Beauregard et al. 1995; Faust et al. 2014b; Peterson and Mooseker 1993).

These data indicate that food grade TiO$_2$ apparently elicits a *bona fide* biological response and not simply a physical artifact as a consequence of in vitro exposure. Estimates based on in vitro exposure suggest that approximately 42 % of microvilli are lost after exposure to food grade TiO$_2$ at the lowest concentration of 350 ng/mL (i.e., 100 ng/cm^2), together these data indicate a need to: (1) identify the aforementioned putative effects of food grade TiO$_2$ with the correct in vivo models that capture cells in their complex social context, (2) identify which physico-chemical parameters influence brush border disruption as the food grade TiO$_2$ employed in this study were both anatase, and (3) identify biological mechanisms by which TiO$_2$ disrupt the brush border since the loss of microvilli results in a decrease in the total surface area of the gut.

References

APHA, AWWA & WEF 2005. Standard Methods for the Examination of Water and Wastewater.

Bachman BJ, Vasile MJ. Ion bombardment of polyimide films. J Vac Sci Technol A Vac Surf Films. 1989;7:2709–16.

Begg DA, Rodewald R, Rebhun LI. The visualization of actin filament polarity in thin sections. Evidence for the uniform polarity of membrane-associated filaments. J Cell Biol. 1978;79:846–52.

Bement WM, Mooseker MS. The cytoskeleton of the intestinal epithelium: components, assembly, and dynamic rearrangements. Cytoskeleton Multi-Vol treat. 1996;3: 359–404.

Bretscher A. Microfilament organization in the cytoskeleton of the intestinal brush border. Cell Muscle Motil. 1983;4:239.

Bretscher A, Weber K. Fimbrin, a new microfilament-associated protein present in microvilli and other cell surface structures. J Cell Biol. 1980a;86:335–40.

Bretscher A, Weber K. Villin is a major protein of the microvillus cystoskeleton which binds both G and F actin in a calcium-dependent manner. Cell. 1980b;20:839–47.

Cho EC, Zhang Q, Xia Y. The effect of sedimentation and diffusion on cellular uptake of gold nanoparticles. Nat Nanotechnol. 2011;6:385–91.

Clark D, Thomas H. Applications of ESCA to polymer chemistry. XVII Systematic investigation of the core levels of simple homopolymers. J Polym Sci Polym Chem Ed. 1978;16: 791–820.

Delpeux S, Beguin F, Benoit R, Erre R, Manolova N, Rashkov I. Fullerene core star-like polymers—1. Preparation from fullerenes and monoazidopolyethers. Eur Polym J. 1998;34: 905–15.

De Beauregard MC, Pringault E, Robine S, Louvard D. Suppression of villin expression by antisense RNA impairs brush border assembly in polarized epithelial intestinal cells. EMBO J. 1995;14:409.

Demri B, Muster D. XPS study of some calcium compounds. J Mater Process Technol. 1995;55:311–4.

Duan Y, Liu J, Ma L, Li N, Liu H, Wang J, et al. Toxicological characteristics of nanoparticulate anatase titanium dioxide in mice. Biomaterials. 2010;31:894–9.

Dunphy Guzman KA, Taylor MR, Banfield JF. Environmental risks of nanotechnology: National nanotechnology initiative funding, 2000–2004. Environ Sci Technol. 2006;40:1401–7.

Faust JJ, Masserano BM, Mielke AH, Abraham A, Capco DG. Engineered nanoparticles induced brush border disruption in a human model of the intestinal epithelium. Nanomaterial. Springer; 2014a.

Faust JJ, Zhang W, Chen Y, Capco DG. Alpha-Fe2O3 elicits diameter-dependent effects during exposure to an in vitro model of the human placenta. Cell Biol Toxicol. 2014b;1–23.

Ferrary E, Cohen-Tannoudji M, Pehau-Arnaudet G, Lapillonne A, Athman R, Ruiz T, et al. In vivo, villin is required for Ca2+-dependent F-actin disruption in intestinal brush borders. J Cell Biol. 1999;146:819–30.

Fröhlich E, Roblegg E. Models for oral uptake of nanoparticles in consumer products. Toxicology. 2012;291:10–7.

Gardner SD, Singamsetty CS, Booth GL, He G-R, Pittman CU. Surface characterization of carbon fibers using angle-resolved XPS and ISS. Carbon. 1995;33:587–95.

Grimm-Günter E-M, Revenu C, Ramos S, Hurbain I, Smyth N, Ferrary E, et al. Plastin 1 binds to keratin and is required for terminal web assembly in the intestinal epithelium. Mol Biol Cell. 2009;20:2549–62.

Heintzelman MB, Mooseker MS. Assembly of the intestinal brush border cytoskeleton. Curr Top Dev Biol. 1992;26:93–122.

Hirokawa N, Cheney RE, Willard M. Location of a protein of the fodrin-spectrin-TW260/240 family in the mouse intestinal brush border. Cell. 1983;32:953–65.

Hirokawa N, Heuser JE. Quick-freeze, deep-etch visualization of the cytoskeleton beneath surface differentiations of intestinal epithelial cells. J Cell Biol. 1981;91:399–409.

Hirokawa N, Tilney LG, Fujiwara K, Heuser JE. Organization of actin, myosin, and intermediate filaments in the brush border of intestinal epithelial cells. J Cell Biol. 1982;94: 425–43.

Howe CL, Mooseker MS. Characterization of the 110-kdalton actin-calmodulin-, and membrane-binding protein from microvilli of intestinal epithelial cells. J Cell Biol. 1983;97: 974–85.

Hu R, Gong X, Duan Y, Li N, Che Y, Cui Y, et al. Neurotoxicological effects and the impairment of spatial recognition memory in mice caused by exposure to TiO2 nanoparticles. Biomaterials. 2010;31:8043–50.

Ishikawa H, Bischoff R, Holtzer H. Formation of arrowhead complexes with heavy meromyosin in a variety of cell types. J Cell Biol. 1969;43:312–28.

Jouan P-Y, Peignon M-C, Cardinaud C, Lemperiere G. Characterisation of TiN coatings and of the TiN/Si interface by X-ray photoelectron spectroscopy and Auger electron spectroscopy. Appl Surf Sci. 1993;68:595–603.

Kalive M, Zhang W, Chen Y, Capco DG. Human intestinal epithelial cells exhibit a cellular response indicating a potential toxicity upon exposure to hematite nanoparticles. Cell Biol Toxicol. 2012;28:343–68.

Koeneman BA, Zhang Y, Westerhoff P, Chen Y, Crittenden JC, Capco DG. Toxicity and cellular responses of intestinal cells exposed to titanium dioxide. Cell Biol Toxicol. 2010;26:225–38.

Lesniak A, Fenaroli F, MONOPOLI MP, Åberg C, DAWSON KA, Salvati A. Effects of the presence or absence of a protein corona on silica nanoparticle uptake and impact on cells. ACS Nano. 2012;6:5845–57.

Lundqvist M, Stigler J, Elia G, Lynch I, Cedervall T, Dawson KA. Nanoparticle size and surface properties determine the protein corona with possible implications for biological impacts. Proc Natl Acad Sci. 2008;105:14265–70.

Milani S, Baldelli Bombelli F, Pitek AS, Dawson KA, Rädler J. Reversible versus irreversible binding of transferrin to polystyrene nanoparticles: soft and hard corona. ACS Nano. 2012;6:2532–41.

Mooseker MS. Organization, chemistry, and assembly of the cytoskeletal apparatus of the intestinal brush border. Annu Rev Cell Biol. 1985;1:209–41.

Mukherjee T, Staehelin L. The fine-structural organization of the brush border of intestinal epithelial cells. J Cell Sci. 1971;8: 573–99.

Oberdörster G, Maynard A, Donaldson K, Castranova V, Fitzpatrick J, Ausman K, et al. Principles for characterizing the potential human health effects from exposure to nanomaterials: elements of a screening strategy. Part Fibre Toxicol. 2005;2:8.

OECD 1994. OECD Guidelines for the Testing of Chemicals, Organization for Economic.

Patterson A. The Scherrer formula for X-ray particle size determination. Phys Rev. 1939;56:978.

Peterson M, Mooseker M. Characterization of the enterocyte-like brush border cytoskeleton of the C2BBe clones of the human intestinal cell line, Caco-2. J Cell Sci. 1992;102: 581–600.

Peterson MD, Bement WM, Mooseker MS. An in vitro model for the analysis of intestinal brush border assembly. II. Changes in expression and localization of brush border proteins during cell contact-induced brush border assembly in Caco-2BBe cells. J Cell Sci. 1993;105:461–72.

Peterson MD, Mooseker MS. An in vitro model for the analysis of intestinal brush border assembly. I. Ultrastructural analysis of cell contact-induced brush border assembly in Caco-2BBe cells. J Cell Sci. 1993;105:445–60.

Powell JJ, Faria N, Thomas-Mckay E, Pele LC. Origin and fate of dietary nanoparticles and microparticles in the gastrointestinal tract. J Autoimmun. 2010;34:J226–33.

Regulations CF. Title 21. Chapter I (revised). 2000;

Revenu C, Ubelmann F, Hurbain I, El-Marjou F, Dingli F, Loew D, et al. A new role for the architecture of microvillar actin

bundles in apical retention of membrane proteins. Mol Biol Cell. 2012;23:324–36.

Schwarz RP, Wolf DA. Rotating bio-reactor cell culture apparatus. 1991;

Shih P, Yung S, Chin T. Thermal and corrosion behavior of P$_2$O$_5$−Na$_2$O−CuO glasses. J Non-Cryst Solids. 1998;224: 143–52.

Stidwill RP, Wysolmerski T, Burgess DR. The brush border cytoskeleton is not static: in vivo turnover of proteins. J Cell Biol. 1984;98:641–5.

Tanuma S, Powell CJ, Penn DR. Calculations of electron inelastic mean free paths. V. Data for 14 organic compounds over the 50–2000eV range. Surf Interface Anal. 1994;21: 165–76.

Tilney LG, Mooseker M. Actin in the brush-border of epithelial cells of the chicken intestine. Proc Natl Acad Sc. 1971;68: 2611–5.

Van Der Flier LG, Clevers H. Stem cells, self-renewal, and differentiation in the intestinal epithelium. Annu Rev Physiol. 2009;71:241–60.

Wang J, Zhou G, Chen C, Yu H, Wang T, Ma Y, et al. Acute toxicity and biodistribution of different sized titanium dioxide particles in mice after oral administration. Toxicol Lett. 2007;168:176–85.

Warheit DB, Hoke RA, Finlay C, Donner EM, Reed KL, Sayes CM. Development of a base set of toxicity tests using ultrafine TiO$_2$ particles as a component of nanoparticle risk management. Toxicol Lett. 2007;171:99–110.

Weir A, Westerhoff P, Fabricius L, Hristovski K, Von Goetz N. Titanium dioxide nanoparticles in food and personal care products. Environ Sci Technol. 2012;46:2242–50.

Weng L, Poleunis C, Bertrand P, Carlier V, Sclavons M, Franquinet P, et al. Sizing removal and functionalization of the carbon fiber surface studied by combined TOF SIMS and XPS. J Adhes Sci Technol. 1995;9:859–71.

Yang Y, Doudrick K, Bi X, Hristovski K, Herckes P, Westerhoff P, Kaegi R. Characterization of food-grade titanium dioxide: presence of nano-size particles. Environ Sci Technol. 2014. doi:10.1021/es500436x.

Zhang W, Kalive M, Capco DG, Chen Y. Adsorption of hematite nanoparticles onto Caco-2 cells and the cellular impairments: effect of particle size. Nanotechnology. 2010;21:355103.